# Noise characteristics of a single sensor camera in digital color image processing

*Tamara Seybold*[†] *Özlem Cakmak*[‡] *Christian Keimel*[‡] *Walter Stechele*[‡] ;
[†] *Arnold & Richter Cine Technik, Türkenstraße 89, 80799 München, Germany*
[‡] *Technische Universität München, Arcisstraße 21, 80333 München, Germany*

## Abstract

*Denoising algorithms are usually tested on standard test images with artificial white Gaussian noise added. This noise model cannot be applied in the denoising of digital images taken with a single sensor camera because of the signal-dependence of the noise, the demosaicking and the color transformations. We study the noise characteristics with respect to the signal domain. Noise distribution and variance are measured in the raw data and approximated using a Gaussian distribution with a variance linearly dependent on the signal. We evaluate the influence of white balance, debayering and the signal domain and calculate the spatial correlation of the noise. In our experiments we both evaluate the influence of the noise characteristics on human perception and on the performance of denoising methods. Based on a subjective test with 18 participants we can show that the spatially correlated camera noise is more visible than the white Gaussian noise and decreases the visual quality of color image sequences significantly. To evaluate the impact of the noise characteristic on denoising, two state-of-the-art denoising methods are applied to our test data. When the noise is signal-dependent and spatially correlated through debayering the peak signal-to-noise ratio (PSNR) decreases by up to 8 dB. We conclude that it is very important to take into account the correct noise characteristics for increasing the visual quality of color image sequences in future research.*

## Introduction

Increasing pixel count driven by the demand for higher resolution, results in a lower pixel pitch in digital image sensors. Thus the amount of light trapped by one pixel is lower and therefore the signal-to-noise ratio decreases. As a high noise level decreases the visual quality of color images and can reduce the efficiency of subsequent image processing tasks, eliminating noise using algorithmic methods is necessary.

The denoising problem has been studied extensively and various methods have been developed [2, 16, 13, 4, 5, 11]. The algorithms are usually optimized using standard test images as the Kodak data set with artificial noise added. The noise model is usually additive white Gaussian noise (AWGN).

A discrepancy exists, though, between the noise model used for testing the algorithms (AWGN) and the real camera noise in digital images. In a typical camera processing, three steps are performed: white balance, demosaicking and color transformations. In the raw data (① in Fig. 1), the image noise is signal-dependent [15]. After debayering the noise is spatially correlated [12] and after the nonlinear color transformations the noise distribution is entirely unknown (② and ③ in Fig. 1). Hence, the noise characteristics in the camera data is fundamentally different from the common AWGN model at all three stages.

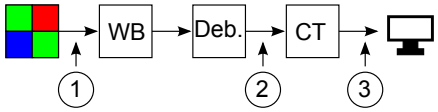


***Figure 1.*** *The Bayer raw data is processed to achieve a display domain image. The three main steps are white balance (WB), Demosaicking (Deb.) and nonlinear color transformations (CT). Denoising can be performed in the display domain ③, in the debayered image ② or in the linear domain directly on the raw data ①.*

Denoising methods for images containing signal-dependent noise have been studied using two different approaches. The first is to include the signal-dependent noise characteristic in the denoising methods. The second strategy is to apply a transformation of the input signal to a signal with approximately constant variance [7, 8, 6]. The methods incorporate signal-dependent but spatially independent noise models which is the case for raw data. However at this level the raw data is mosaicked in real single sensor camera images, so that denoising methods must be adapted accordingly. There are different approaches of denoising mosaicked data using the traditional noise model [9, 19, 17, 3], but there are two problems with denoising in the raw domain: it requires adapting the methods to the lack of neighboring pixels of the same color, which can be complex. The second problem though is the signal domain of the raw images. Before color processing the raw image is a signal proportional to the light level (linear domain, ① in Fig. 1). To display the image on a monitor demosaicking and nonlinear color transformations have to be applied to convert the signal to the display domain (③ in Fig. 1). The color processing can only be done after demosaicking because all three color components are needed for the transformations. Therefore denoising raw data would require coping with the linear domain signals, signal-dependent noise and missing values.

A combined study of the noise characteristics in images taken with a single sensor camera must consider all three aspects: signal-dependence, debayering and the signal domain. We will evaluate the noise characteristics with respect to the signal domain and work out the differences between the real camera noise in digital color images and the traditional noise model. To evaluate the impact of these differences we compare the visual quality of noisy images using both noise models based on a subjective test, which enables us to discuss the impact of the noise model on human perception. Additionally we show how the noise characteristic influences denoising results.

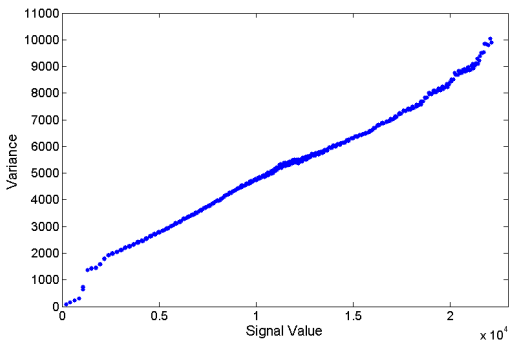


(a)

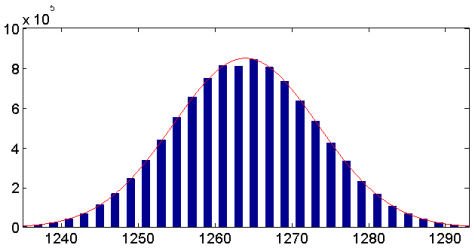


(b)

***Figure 2.*** *Variance and distribution of sensor noise*

The structure of this paper is as follows. First, the characterization of camera noise in the raw domain is described. We subsequently show the difference between the raw domain and the display domain. We describe the processing of the raw images and the relevance of the processing steps to the noise characteristics. We then evaluate the noise characteristics after the processing, in particular the spatial correlation in the display domain. The visual perception of different noise types is analyzed based on a subjective test. Finally, we apply denoising to a simulated video sequence with different noise types, thus we can evaluate the effect of different noise characteristics on denoising results.

## Camera Noise Characteristics

To measure the camera noise in the raw images at different signal levels we take a series of exposures with the ARRI Alexa camera. This camera is developed for motion picture in digital cinema. The Alexa camera has a CMOS sensor with a resolution of $2880 \times 1620$. The sensor read out provides two different paths with different amplification (dual gain read out). The low amplified or the high amplified path is chosen according to the signal level. This enhances the low light performance of the camera. In front of the sensor the Alexa camera has filter pack composed by an infrared cut-off filter, an ultraviolet cutoff filter and a low pass filter to reduce aliasing. Between the filter pack and the sensor there is the Bayer color filter array.

To measure the camera noise we use the photon transfer method [1]. Two frames $A$ and $B$ are used to calculate the variance as the sum of the squared differences in the active area of size $N \times M$.

$$\sigma^2 = \frac{1}{2NM} \sum_{i=0}^{M-1} \sum_{j=0}^{N-1} (A_{ij} - B_{ij})^2 \tag{1}$$

The curve in Fig. 2(a) shows the variance plotted over the respective mean value. The signal value is the digital 16bit value of the sensor output which represents the light intensity level. The variance of the sensor noise can be approximated by a linear curve. This result matches the results with other cameras in [15]. There is one difference though. The relationship is only partially linear, because of the sensors dual gain read out. The two read out paths are combined in the region around signal value $0.1 \times 10^4$. This explains the step in the variance curve. We can see that the dual gain architecture reduces the read-out-noise.

In Fig. 2(b) we show the distribution at a fixed signal level. The distribution is very similar to the Gaussian distribution. That means we can well approximate the sensor noise using a Gaussian distribution with signal-dependent variance. $x_n = x + n$ with $n \sim \mathcal{N}(0, \sigma(x))$ and $\sigma(x) = \sqrt{mx+t}$ where $m$ is the slope and $t$ the intercept of the linear approximation of the curve in Fig. 2(a). Because of the dual gain read out the values for $m$ and $t$ depend on the signal region.

As we have Bayer data at this point, the noise level of course depends on the signal value of one color. With different signal values of R, G and B, the variance of neighboring pixels is quite different depending on the color in the image.

## Camera Noise in the processing pipeline

As explained in the introduction the raw data is in the linear domain, i.e. the signal value is proportional to the amount of light collected by the sensor. When processing the sensor output multiple steps are performed to achieve a monitor color image. The steps are

1. White Balance,
2. Debayering,
3. Color Transformations.

Applying these steps gives a displayable image, but they also influence the sensor noise.

White balance is a known gain factor $g_c$ different for each color. It directly influences the noise $n_c$ in the different colors.

$$n_{wb} = g_c n_c \tag{2}$$

The white balance changes the noise level of the different channels. As most algorithms adjust the parameters depending on the noise level, denoising algorithms can be adapted to the different level.

The next step is to create a color image with three color values per pixel by demosaicking the Bayer image $I_b$. Different debayering algorithms can be used and the noise characteristic is changed depending on the algorithm. As high performance debayering algorithms are nonlinear and use neighboring values the transformation $D$ will be used as a general description. $D$ depends on the color $c$, because the amount and position of neighboring pixel is different for red/blue and green. Usually it also depends on the neighboring pixels in a window $w$ around the pixel being interpolated.

$$n_{deb} = D_c\left(n_{wb}, w(I_b)\right) \tag{3}$$

The debayering step creates three color values by interpolation using the pixel and the neighbor values. Therefore, a spatial and

**Table 1. Correlation Matrices for different debayering methods, calculated using AWGN and the Kodak data set. While in the usual uncorrelated noise model the noise values don't correlate with the neighboring values and thus lead to a matrix with only a one in the upper left matrix position, these correlation matrices show that a strong correlation to the neighboring pixels is present after debayering.**

| $C_{bilin} =$ | $C_{dlmmse} =$ | $C_{lu} =$ |
|---|---|---|
| $\begin{bmatrix} 1 & 0,5693 & 0,1243 \\ 0,5715 & 0,3214 & 0,07181 \\ 0,1284 & 0,07425 & 0,0191 \end{bmatrix}$ | $\begin{bmatrix} 1 & 0,2239 & -0,0066 \\ 0,375 & 0,06351 & 0,03626 \\ -0,003771 & 0,03715 & 0,03545 \end{bmatrix}$ | $\begin{bmatrix} 1 & 0,3173 & 0,01578 \\ 0,2947 & 0,1007 & 0,04422 \\ 0,01689 & 0,04548 & 0,04233 \end{bmatrix}$ |

chromatic correlation of the three color channels is introduced. The spatial correlation of the noise $n_{deb}$ in the debayered image is usually disregarded in common state-of the art denoising methods.

The third step, the color transformations, is a nonlinear tone mapping and color space conversion to map the linear values to displayable signals. Color transformations can strengthen the spatial and chromatic correlation. The exact way color conversion is done is an individual choice and their discussion would go beyond the scope of this paper. The debayering is a necessary step to obtain a color image and it introduces the spatial correlation, therefore we focus on the debayering in the next section.

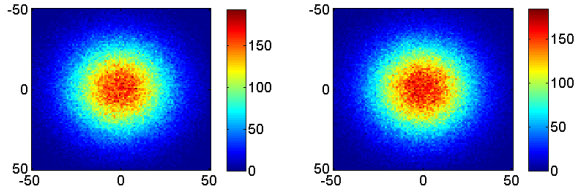

(a) No debayering

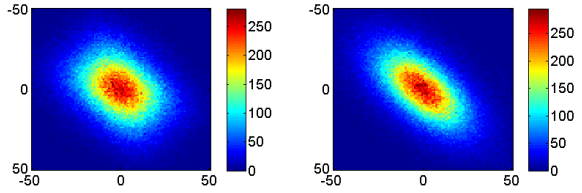

(b) Bilinear

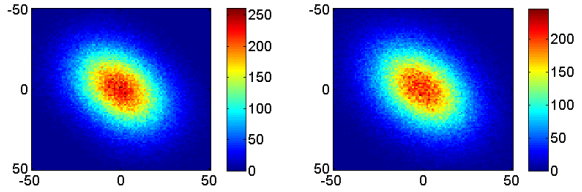

(c) Lu/Tan debayering

***Figure 3.*** *Scatter Plot of the noise in a noisy Kodak image before (a) and after debayering (b,c); the first Kodak image was used and AWGN with $\sigma = 20$ added. From left to right the G and B channel. The R channel is not shown, because as the demosaicking methods interpolate the B and R channels the same way and the scatter plots of B and R look very similar.*

## Local Correlation introduced with Debayering

To evaluate the influence of debayering for different methods we first use the standard test images from Kodak. This choice is due to the fact that most debayering algorithms in literature are optimized using that test set.

The spatial correlation of the noise is evaluated after demosaicking a noisy and a noise-free image. The difference image contains the error introduced by the noise. We use this difference image to calculate the correlation matrix $C$ and a scatter plot. We compare different debayering algorithms and their influence on the noise characteristics.

To visualize the distribution we plotted 2-dimensional histograms of the noise. The difference of the noisy and the reference image is the error due to noise. In the 2D-histogram the densities of two neighboring pixels are plotted. The color represents the density; the position in the plot represents the value of the error. The resulting scatter plots for an image with AWGN without debayering are given in Fig. 3(a). The distribution is symmetric as expected for uncorrelated noise. Fig. 3(b) and 3(c) show the scatter plots of the noise after demosaicking using bilinear interpolation and using the debayering method proposed by Lu/Tan [10]. The scatter plots of the debayered noise are dispersed into the diagonal direction, which indicates a correlation: it is more likely for a pixel to have the same or a similar value as its neighbors.

In the last section we discussed the influence of processing on the noise. An additive model for the noisy image $I_n$ is to be the sum of the image $I$ and the noise $n$. For denoising applications it is quite usual to assume white Gaussian noise,

$$I_n = I + n; \;\; n \sim \mathcal{N}(0, \sigma) \tag{4}$$

spatially independent with a fixed variance $\sigma$. This assumption is far from real camera noise, which is correlated spatially and signal-dependent. We calculated the correlation matrices $C$, given in Tab. 1. The matrices contain the correlation between a pixel $(i, j)$ and its neighbors; more precisely the entry $(k, l)$ in the matrix corresponds to the correlation of the neighbor pixel $(i+k, j+l)$. Numbers for bilinear interpolation, DLMMSE [18], and Lu und Tan method [10] are given. The matrices are $3 \times 3$ because numbers outside of this regions are very small. The bilinear interpolation has the strongest correlation.

We propose to approximate the noise after debayering by a

***Figure 4.*** *One frame of the computer-generated test sequence*

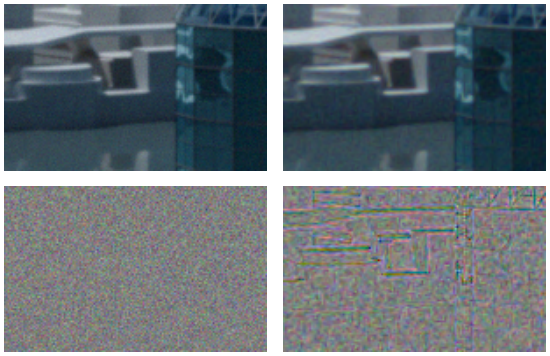

***Figure 5.*** *Crop of the sequence "City". Noisy image (left) and noisy image with debayering (right). In the second row the respective difference image $I_d$ scaled for display ($I_{d,scaled} = I_d \cdot 4 + 128$).*

multivariate Gaussian distribution with a covariance matrix $\Sigma$.

$$I_n \approx I + n;\ \ n \sim \mathcal{N}(0, B\Sigma_d B^T) \qquad (5)$$
$$\text{with } \Sigma = B\Sigma_d B^T$$

We expect the expression to be separable with a diagonal matrix $\Sigma_d$ whose entries linearly depend on the corresponding pixel intensities (c.f. Fig. 2(a)) and a matrix $B$ depending on the spatial correlation introduced by the debayering. For linear debayering methods the above approximation is exact.

The color transformations can strengthen the correlation. As the color transformations are an individual choice, we leave that topic to future research.

## Visual Perception of spatially correlated noise

While we discussed the different characteristics of realistic camera noise in the last sections, we now evaluate the human perception of the noise. We use computer-generated video sequences combined with a simulation of the camera parameters.

The "city" sequence is a pan over a city, see Fig. 4. The frames are rendered in high resolution and in linear signal domain. To incorporate the optic of a camera system the images are multiplied in the Fourier domain with the optical transfer function of the camera. This step takes into account the diffraction limited lens, the optical low pass filter and the pixel aperture, as described by Schöberl et al. [14]. The images used in a test to compare the different noise types are simulated with the signal-dependent camera noise and compared to the traditional model, AGWN. The camera noise is added in linear domain according to the measured values using a Gaussian distribution with a signal-dependent variance defined by the linear approximation of the measurement data. This gives us simulated raw images with a reference.

To compare the effect of debayering on the noise characteristic, the image processing with debayering is compared to the processing without debayering. The last one is only possible with the simulated RGB values; in real raw images the debayering cannot be omitted. A crop of the city sequence with noise and with/without debayering is shown in Fig. 5. The degraded image (noisy, with and without debayering) is compared to the reference. The difference of the noisy image to reference image, shown in Fig. 5, visualize the effect: When debayering is included the noise is structured and of coarser grain. The difference images are scaled the same way to be comparable. We also observe that the correlated noise after debayering appears more colorful. This may be caused by the lower frequency of the signal. As the maximum of the luminance contrast sensitivity is in higher frequencies, the color might be perceived stronger for a low-frequency signal.

To obtain reliable information about the human perception of the different noise characteristics, we perform a subjective test with 18 participants. We used the double stimulus DSIS methodology with a undistorted reference and impaired noisy sequence according to ITU-R BT.500. A discrete scale from 1 to 10, representing a impairment range of "very annoying" to "imperceptible", was used. The task for the participants was to assess the perceived impairment of the images. The test was performed in the ITU-R BT.500 compliant video quality evaluation laboratory at the Institute for Data Processing at Technische Universität München. For displaying the videos, a color calibrated Sony BVM-L230 reference LCD display with a screen diagonal of 23 inches was used. To get reliable results, the outlier were removed in the post processing of the subjects' votes. Votes were removed, if they deviated more than $2\sigma$ from the mean for a sequence. Using this criterion, 4.6% of all votes were discarded. After outlier removal, the mean opinion score (MOS) was determined for the different test images.

The MOS provides reliable values for the subjective quality of the test images. Four different noise models were used in our test: the usual AWGN model, AWGN with demosaicking, signal-dependent noise without demosaicking and finally the realistic camera noise model – signal-dependent noise with demo-

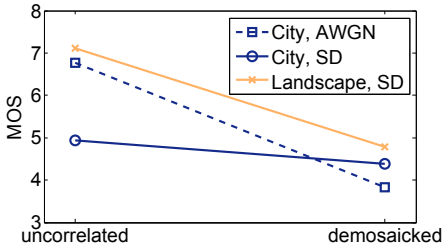


***Figure 6.*** *The MOS results for the test sequences "City" and "Landscape" using the traditional AWGN model (dashed) and the realistic signal-dependent noise (solid lines). The uncorrelated noise, processed without demosaicking, is shown on the left, the results with demosaicking on the right.*

**Table 2. PSNR results for denoising the city sequence with BM3D [4] and BLS-GSM [13]. Two noise types are used: Gaussian noise added in display domain (AWGN) and signal-dependent camera noise added in linear domain (SD). Denoising is either performed in linear domain (②) or in display domain (③), numbers as in Fig. 1.**

| | Noisy | | BLS-GSM | | BM3D | |
|---|---|---|---|---|---|---|
| | RGB | dem. | RGB | dem. | RGB | dem. |
| AWGN /③ | 35,51 | 35,35 | 44,47 | 38,81 | 46,33 | 38,17 |
| SD /③ | 31,51 | 33,95 | 36,45 | 37,43 | 43,11 | 39,49 |
| SD /② | 31,51 | 33,95 | 39,40 | 36,61 | 41,99 | 38,34 |

saicking. Based on the MOS, we evaluate the visual quality of the noisy test sequences and analyze the main differences between the realistic camera noise and AWGN: spatial correlation introduced through demosaicking and signal-dependence.

The spatially correlated noise is perceived as more annoying. While the MOS is different depending on image content and noise type, Fig. 6 shows a lower MOS for the all the demosaicked sequences compared to the sequences with uncorrelated noise. This may be due to the higher visibility of spatially correlated noise, which shows coarser grain and appears more colorful. The MOS of the city sequence with AWGN is about 3 scores lower when demosaicking is included. Regarding the sequences with signal-dependent noise, the MOS is 0.5 lower for the city sequence and 2.3 lower for the landscape sequence when demosaicking is included. We thus showed the significant effect of the noise characteristic on the visual perception of color video sequences: the spatial correlation of the noise decreases the perceived image quality. In the next section we will discuss the impact of the noise characteristic on denoising.

## Influence on Denoising

To answer the question what impact the difference between the traditional independent noise and the camera noise has, we want to evaluate the effect on denoising in this section. We already showed that the spatially correlated noise is more disturbing, thus reduces the visual quality. We thus can expect that the visual quality is also reduced with debayering when rating the denoising results. To evaluate if there is also an effect on the denoising error, we use the PSNR, as it directly measures the error of the denoised image quantitatively.

The PSNR of the denoising results is shown in Tab. 2. We compare signal-dependent camera noise with a variance as in Fig. 2(a), to Gaussian noise added in display domain. The variance of the Gaussian noise was fixed with the objective of similar visual impression in display domain. We process the frames in two ways: without debayering (called "RGB" in Tab. 2) and with debayering ("dem." in Tab. 2). All these cases then are denoised, either in linear domain (②) or in display domain (③ in Fig. 1). Two different denoising algorithms are used: BLS-GSM [13] and BM3D [4]. The parameters are picked to obtain the most visually pleasing results. We calculated the PSNR of each frame and took the mean over 20 frames.

While the visual quality in the last section was shown to be lower with demosaicking, the PSNR of the noisy sequence shows that the demosaicking has a slight denoising effect, which leads to a higher PSNR of the debayered noise. However, the PSNR of denoised images is up to 8 dB lower when the demosaicking is included and thus the noise correlated. Hence denoising is significantly harder due to the spatial correlation in the debayered images. BLS-GSM denoising brings lower PSNR improvement for the signal-dependent noise, thus it shows similar to the noisy case a slightly higher PSNR with the demosaicked noise. BM3D seems to be more robust to the signal-dependence, for both it leads to an improvement of above 10 dB in PSNR, but it seems more sensitive to the spatially correlated noise as the improvement of 5,54 dB for AWGN and 2,82 dB for signal-dependent noise is much smaller.

BLS-GSM works better in linear domain, we think because the noise characteristics differ less from the assumed model. In contrast the similarity based method, BM3D, works better in display domain. Thus denoising methods have to be tested on linear domain data explicitly and it depends on the methods if denoising in the linear domain or in the display domain works better.

In total the results show that it is very important to adapt the standard methods to the correct noise model.

## Conclusion

Camera Noise in raw data can be modeled as a Gaussian distribution with signal-dependent variance, but the camera noise characteristic in display domain images is very different from the noise in the raw domain because of its spatial correlation introduced by debayering. Correlation matrices were calculated for different debayering methods using standard test images. Using a computer generated test sequence that includes the optical characteristics of the camera we evaluate the impact of the noise characteristic on the denoising performance. Camera noise is compared to the traditional model and the influence of debayering is studied. We can conclude that the spatially correlated noise is perceived as more annoying: in our subjective test with 18 participants the visual quality was rated significantly lower for the sequences containing correlated noise. Denoising was applied to the same test data, and we showed that the PSNR of the denoising results is up to 8 dB lower with correlated camera noise. Hence the noise characteristic in the image has a significant effect on both visual perception and on denoising results. To account for the correct noise model is thus very important to achieve high image quality in future research.

## References


[1] Standard for characterization of image sensors and cameras. EMVA Standard 1288, 2010.

[2] A. Buades, B. Coll, and J. Morel. A review of image denoising

algorithms, with a new one. *Multiscale Modeling & Simulation*, 4(2):490 – 530, 2005.

[3] L. Condat. A simple, fast and efficient approach to denoisaicking: Joint demosaicking and denoising. In *Image Processing (ICIP), 2010 17th IEEE International Conference on*, pages 905 – 908, sept. 2010.

[4] K. Dabov, A. Foi, V. Katkovnik, and K. Egiazarian. Image denoising by sparse 3-d transform-domain collaborative filtering. *Image Processing, IEEE Transactions on*, 16(8):2080 – 2095, aug. 2007.

[5] M. Elad and M. Aharon. Image denoising via learned dictionaries and sparse representation. In *Computer Vision and Pattern Recognition, 2006 IEEE Computer Society Conference on*, volume 1, pages 895 – 900, june 2006.

[6] A. Foi. Clipped noisy images: heteroskedastic modeling and practical denoising. *Signal Processing*, pages 2609 – 2629, 2009.

[7] A. Foi, V. Katkovnik, and K. Egiazarian. Signal-dependent noise removal in pointwise shape-adaptive DCT domain with locally adaptive variance. In *Proceedings of the 15th European Signal Processing Conference, EUSIPCO*, 2007.

[8] R. Giryes and M. Elad. Sparsity based poisson denoising. In *2012 IEEE 27th Convention of Electrical Electronics Engineers in Israel (IEEEI)*, pages 1 – 5, nov. 2012.

[9] K. Hirakawa and T. W Parks. Joint demosaicing and denoising. *Image Processing, IEEE Transactions on*, 15(8):2146 – 2157, aug. 2006.

[10] W. Lu and Y.-P. Tan. Color filter array demosaicking: new method and performance measures. *Image Processing, IEEE Transactions on*, 12(10):1194 – 1210, oct. 2003.

[11] J. Mairal, F. Bach, J. Ponce, G. Sapiro, and A. Zisserman. Non-local sparse models for image restoration. In *Computer Vision, 2009 IEEE 12th International Conference on*, pages 2272 – 2279, 2009.

[12] S. H. Park, H. S. Kim, S. Lansel, M. Parmar, and B.A. Wandell. A case for denoising before demosaicking color filter array data. In *Signals, Systems and Computers, 2009 Conference Record of the Forty-Third Asilomar Conference on*, pages 860 – 864, nov. 2009.

[13] J. Portilla, V. Strela, M. J Wainwright, and E. P Simoncelli. Image denoising using scale mixtures of gaussians in the wavelet domain. *Image Processing, IEEE Transactions on*, 12(11):1338 – 1351, nov. 2003.

[14] M. Schöberl, W. Schnurrer, A. Oberdörster, S. Fößel, and A. Kaup. Dimensioning of optical birefringent anti-alias filters for digital cameras. In *Image Processing (ICIP), 2010 17th IEEE International Conference on*, pages 4305 – 4308, sept. 2010.

[15] H. J. Trussell and R. Zhang. The dominance of poisson noise in color digital cameras. *Image Processing (ICIP), 2012 19th IEEE International Conference on*, 2012.

[16] E. Vansteenkiste, D. Weken, W. Philips, and E. Kerre. Perceived image quality measurement of state-of-the-art noise reduction schemes. In J. Blanc-Talon, W. Philips, D. Popescu, and P. Scheunders, editors, *Advanced Concepts for Intelligent Vision Systems*, volume 4179 of *Lecture Notes in Computer Science*, pages 114 – 126. Springer Berlin Heidelberg, 2006.

[17] L. Zhang, R. Lukac, X. Wu, and D. Zhang. PCA-Based spatially adaptive denoising of CFA images for single-sensor digital cameras. *Image Processing, IEEE Transactions on*, 18(4):797 – 812, apr. 2009.

[18] L. Zhang and X. Wu. Color demosaicking via directional linear minimum mean square-error estimation. *Image Processing, IEEE Transactions on*, 14(12):2167 – 2178, dec. 2005.

[19] L. Zhang, X. Wu, and D. Zhang. Color reproduction from noisy cfa data of single sensor digital cameras. *Image Processing, IEEE Transactions on*, 16(9):2184 – 2197, sept. 2007.

## Author Biography

*Tamara Seybold received her B.Sc degree and her Dipl.-Ing. (M.Sc) degree in electrical engineering and information technology in 2009 and 2011, both from the Technische Universität München (TUM), Munich, Germany. She has been a Digital Imaging Scientist at Arnold & Richter Cine Technik (ARRI) since 2012. She additionally is a PhD candidate at the Institute for Integrated Systems at TUM and her research is focused on efficient denoising of color image sequences.*

*Özlem Cakmak received her B.Sc degree degree in electrical engineering and information technology in 2012. She is a M.Sc. student at the TUM. In her B.Sc. thesis she worked on the influence of debayering algorithms on noise characteristics.*

*Christian Keimel received the B.Sc., Dipl.-Ing. and Dr.-Ing. degree in electrical engineering and information technology from the TUM, in 2005, 2007 and 2014, respectively. His research interests include subjective and objective video quality assessment.*

*Walter Stechele received the Dipl.-Ing. and Dr.-Ing. degrees in electrical engineering from the TUM, in 1983 and 1988, respectively. In 1990 he joined Kontron Elektronik GmbH, a German electronic company, where he was responsible for the ASIC and PCB design department. Since 1993 he has been Academic Director at the Institute for Integrated Systems at the TUM. His interests include visual computing and robotic vision, with focus on Multi Processor System-on-Chip (MPSoC) architectures and design methodology, low power optimization, dynamic reconfiguration of FPGA devices, and applications in automotive and robotics.*